

# Infrared Spectrum of Matrix-Isolated Hexamethylenetetramine in Ar and H<sub>2</sub>O at Cryogenic Temperatures

Max P. Bernstein,<sup>1</sup> Scott A. Sandford,\* Louis J. Allamandola, and Sherwood Chang

NASA–Ames Research Center, Mail Stop 245–6, Moffett Field, California 94035-1000

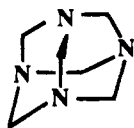
Received: July 15, 1994; In Final Form: September 13, 1994<sup>⊗</sup>

The infrared spectra of hexamethylenetetramine (HMT) isolated in an argon matrix at 12 K, frozen in H<sub>2</sub>O at temperatures from 12 to 200 K, and as a pure solid, are reported. The results of ultraviolet photolysis of matrix-isolated HMT and HMT frozen in H<sub>2</sub>O ice are also presented, and implications for infrared astronomy and astrochemistry are discussed. Furthermore, a simple technique for incorporating large nonvolatile organic molecules into a matrix is described.

## Introduction

Laboratory infrared spectra of organic molecules taken under appropriate astrophysical conditions (low temperature, high vacuum, and frozen into mixed molecular ices) are essential for the assignment of spectral bands caused by organic species in the spectra of comets and dust in the interstellar medium. Unfortunately, few complex organic molecules have been studied under conditions relevant to astronomy.

Hexamethylenetetramine (HMT), C<sub>6</sub>H<sub>12</sub>N<sub>4</sub>, has been known for over 130 years.<sup>2</sup> It was the first organic molecule on which X-ray crystallography was performed, and it was found to have tetrahedral symmetry.<sup>3</sup> The infrared (IR) and Raman spectra of the solid<sup>4</sup> and infrared spectra of the gas<sup>5</sup> have been reported, and the small number of observed fundamentals is indicative of the high degree of symmetry of this molecule. The IR spectral properties and photochemistry of HMT, especially frozen in H<sub>2</sub>O ice, are of astronomical interest, as it may comprise a portion of interstellar ice grains, icy satellites, and the organic crust of comets.<sup>6–9</sup>



HMT

## Experimental Section

The technique and apparatus employed here are typical of those used in matrix isolation studies. As they have been described in detail elsewhere,<sup>10</sup> only the salient points will be reviewed here. A CsI substrate is suspended in a chamber under ultrahigh vacuum ( $\sim 10^{-8}$  mbar) prior to sample deposition. Gas samples are frozen onto the CsI window cooled to 12 K by a closed cycle helium refrigerator. The infrared spectra were measured using a Nicolet 7000 FTIR spectrometer at 0.9 cm<sup>-1</sup> resolution (the observed fwhm of an unresolved feature). Because of oversampling (2 points per resolution element), reported band positions are accurate to  $\pm 0.2$  cm<sup>-1</sup>.

Ultraviolet (UV) radiation was generated by a microwave-powered, hydrogen-flow, discharge lamp typically operated at 70 W and equipped with a MgF<sub>2</sub> window. The hydrogen pressure is held at 100 mTorr by continuous pumping on the lamp while hydrogen is injected at a controlled rate. Under these conditions the flux is evenly divided between the Lyman  $\alpha$  line at 1216 Å and a  $\sim 200$  Å wide collection of molecular

transitions centered at about 1600 Å. The total flux produced by the lamp is  $\sim 2 \times 10^{15}$  photons/(cm<sup>2</sup> s).<sup>11</sup>

Argon (Matheson 99.999% pure) was passed through a liquid nitrogen cooled trap to remove condensable contaminants and used without further purification. H<sub>2</sub>O (distilled) was purified by three freeze–pump–thaw cycles before use. The hexamethylenetetramine (HMT), C<sub>6</sub>H<sub>12</sub>N<sub>4</sub> (Fischer Scientific 99.9% pure; kindly provided by Dr. B. N. Khare of Cornell University), was gently warmed while under vacuum at 10<sup>-6</sup> mbar before use.

Matrices containing HMT were prepared by the technique used by Hudgins *et al.* to produce inert gas matrices containing polycyclic aromatic hydrocarbons.<sup>12</sup> Deposition of HMT vapor onto the cooled substrate was achieved as follows: HMT was placed into a clean, dry, 12 cm long straight 0.5 in. o.d. Pyrex tube, with a greaseless glass (Ace glass 8194–69 0–10 mm) stopcock near one end. The open end of the tube was inserted into the vacuum chamber through a 0.5 in. Cajon ultra-torr fitting which had been silver soldered onto the stainless steel faceplate of the vacuum chamber. A 0.5 in. hole had been bored through the faceplate to allow the end of the glass tube to sit flush with the internal face of the vacuum chamber. Pure HMT was deposited onto the cold window by simple sublimation of the solid HMT at room temperature from the Pyrex tube with the greaseless, glass stopcock open to the first mark (1 mm). The production of HMT isolated in an argon matrix was achieved by cocondensing HMT onto the CsI window while argon was simultaneously deposited through a separate calibrated copper inlet tube. The argon flow was adjusted using a separate valve to a rate ( $\sim 10$  mm/h) that provided good isolation of the HMT. Since the HMT and argon were deposited through separate ports, the exact ratio of Ar to HMT is not known. However, based on the rate of argon flow and assuming the integrated absorbance value of the 1007.3 cm<sup>-1</sup> band of pure solid HMT ( $A = 5.0 \times 10^{-18}$  cm/molecule)<sup>9</sup> is appropriate for the 1011.2 cm<sup>-1</sup> band produced by HMT in argon, we estimate  $M/R \approx 500$ –1000. Sample deposition times of 10–15 min were adequate to produce a 1011.2 cm<sup>-1</sup> feature having an absorption depth of 20–30%. The HMT was deposited in an astrophysically relevant H<sub>2</sub>O-rich ice in the same manner, using H<sub>2</sub>O vapor in place of argon (flow rate = 0.04 mm/h). Based on the relative strengths of the H<sub>2</sub>O band near 3250 cm<sup>-1</sup> and the 1013.1 cm<sup>-1</sup> HMT band, we estimate  $M/R \approx 3$  for our HMT–H<sub>2</sub>O experiments.

<sup>⊗</sup> Abstract published in *Advance ACS Abstracts*, November 1, 1994.

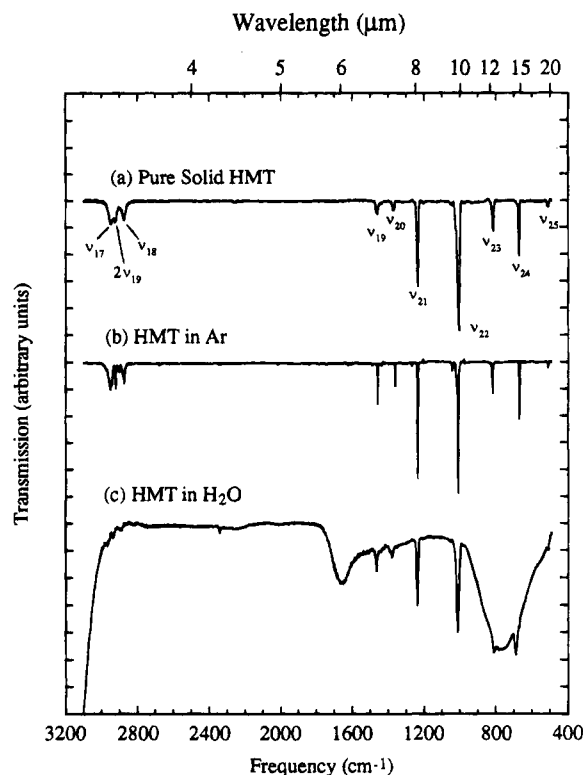


**Figure 1.** 3200–400  $\text{cm}^{-1}$  infrared spectra of (a) solid HMT at 12 K (assignments taken from Bertie and Solinas<sup>4</sup>), (b) HMT isolated in an argon matrix 12 K ( $M/R \approx 500$ –1000), and (c) HMT frozen in  $\text{H}_2\text{O}$  at 12 K ( $M/R \approx 3$ ).

## Results and Discussion

**Spectra.** The infrared spectrum of solid HMT at 12 K (Figure 1a) is quite similar to that previously reported for the solid at 100 K<sup>4</sup>. The spectrum of HMT isolated in an argon matrix (Figure 1b) differs from that of the solid at 12 K in a few respects. Many of the weaker features evident in the spectrum of matrix-isolated HMT are not seen in the spectrum of solid HMT or are only visible if the stronger bands are saturated (see Table 1). Of the stronger features common to both spectra, only two of the bands in the spectrum of pure HMT are shifted more than 4  $\text{cm}^{-1}$  relative to those produced by Ar-matrix-isolated HMT (Table 1, Figure 1a–b).

In contrast, greater spectral perturbations occur when HMT is frozen in an astrophysically relevant  $\text{H}_2\text{O}$  ice at 12 K (Table 1, Figure 1c). Many of the bands observed in the argon-isolated spectrum are obscured by the strong  $\text{H}_2\text{O}$  absorptions. As expected, HMT bands that are observed in the spectrum of the  $\text{H}_2\text{O}$  ice mixture are displaced relative to the argon matrix values to a greater extent than that of solid HMT (see Table 1). The largest shifts between the spectrum of argon-matrix-isolated HMT and that of HMT frozen in  $\text{H}_2\text{O}$  generally occur for features associated with H atom motions, but the CNC deformation is also strongly affected. The most affected bands of HMT in  $\text{H}_2\text{O}$  fall at  $\sim 2966$ ,  $\sim 2935$ ,  $\sim 2892$ , 1380.3, 809.1, and 689.6  $\text{cm}^{-1}$  (shifted from the argon values by +14.4, +12.3, +16.0, +17.3, –10.0, and +19.9  $\text{cm}^{-1}$ , respectively) and involve the asymmetric  $\text{CH}_2$  stretch ( $\nu_{17}$ ),  $\text{CH}_2$  deformation ( $\nu_{19}$ ), symmetric  $\text{CH}_2$  stretch ( $\nu_{18}$ ),  $\text{CH}_2$  wag ( $\nu_{20}$ ),  $\text{CH}_2$  rock ( $\nu_{23}$ ), and CNC deformation ( $\nu_{24}$ ), respectively.<sup>4</sup>

**Annealing.** Warming solid HMT from 12 to 200 K had little effect on the positions of the major bands, but did cause changes in relative band intensities. For example, the 2948.9 and 2923.9  $\text{cm}^{-1}$  bands in the 12 K spectrum of solid HMT were observed to steadily diminish relative to the 2874.4  $\text{cm}^{-1}$  band on warming from 12 to 200 K. In addition, the seven prominent

**TABLE 1: Hexamethylenetetramine Peak Positions and Assignments<sup>a</sup>**

vibrational assignment	pure HMT position	HMT–Ar position	HMT– $\text{H}_2\text{O}$ position
$\nu_{25}$ CNC deformation	510.5 w	510.6 w	508.9 w
$\nu_{24} - \nu_L^b$	659.5 w sh	658.6 w	668.3 w
$\nu_{24}$ CNC deformation	670.9 s	669.7 s	689.6 m
$\nu_{24} + \nu_L^b$	681.7 sh	701.3 w	
$\nu_{23}$ $\text{CH}_2$ rock	777.9 w	811.9 w sh 815.3 w sh	809.1 w
$\nu_{23}$ $\text{CH}_2$ rock	815.0 m	819.1 m	
$\nu_{10} + \nu_{16}$	$\sim 818$ sh	820.5 sh 824.5 w 831.2 sh 833.7 w 850.4 vw	
$\nu_{23} + \nu_L, \nu_{16} + \nu_{25}, \nu_{23} + \nu_L^b$	932.5 w	974.4 w 1002.4 sh	
$\nu_{22}$ CN stretch	1007.3 vs	1011.2 vs 1015.7 sh	1013.1 vs
$2\nu_{25}$	$\sim 1020$ sh	1021.2 sh 1022.4 sh 1033.1 vw	
$\nu_{16} + \nu_{24}$	1040.9 w	1041.5 w sh	
$\nu_{10} + \nu_{24}$	1044.8 w	1044.3 w	1053.6 w
$\nu_{24} + \nu_{25}$	1129.3 w 1192.4 w	1128.1 w 1193.3 w 1231.4 sh	
$\nu_{21}$ CN stretch	1234.3 s	1237.6 vs 1269.5 w	1239.9 s
$\nu_{10} + \nu_{23}$		1363.0 m	
$\nu_{20}$ $\text{CH}_2$ wag	1368.3 m	1365.4 sh 1365.4 sh	1380.3 m
$\nu_9 + \nu_{16}$	1393.4 vw	1394.5 w	1391.3 sh
$\nu_{15} + \nu_{25}$	1435.8 w	1437.6 w	
$\nu_4 + \nu_{24}, 2\nu_{10} + 2\nu_{25}$	1440.6 vw		1444.5 sh
$\nu_{19}$ $\text{CH}_2$ deformation	1460.7 m	1458.9 m	1465.5 m
$\nu_{23} + \nu_{24}$	1485.5 w	1490.7 w	
$\nu_{18}$ sym $\text{CH}_2$ stretch	2874.4 m	2875.4 m 2881.0 sh 2886.4 sh 2900.0 w 2902.8 sh	$\sim 2892^c$
$2\nu_{19}, \nu_2 + \nu_{19}$	2923.9 m	2922.7 m 2943.4 sh 2947.9 sh	$\sim 2935^c$
$\nu_{17}$ asym $\text{CH}_2$ stretch	2948.9 m	2951.6 m 2959.5 sh 2974.8 w	$\sim 2966^c$

<sup>a</sup> All samples at 12 K, positions given in  $\text{cm}^{-1}$ . Band assignments, using Herzberg's convention, apply strictly to pure HMT and are taken from studies of the solid by Bertie and Solinas.<sup>4</sup> <sup>b</sup>  $\nu_L$  refer to lattice modes. <sup>c</sup> The positions and widths of these bands are difficult to determine due to overlap with the strong O–H stretching band of  $\text{H}_2\text{O}$  centered near 3250  $\text{cm}^{-1}$ .

bands below 1600  $\text{cm}^{-1}$  all deepened and sharpened with increasing temperature. This is a common spectral behavior for material changing from an amorphous solid to a more ordered crystalline phase.

Warming of HMT–Ar samples resulted in the loss of the matrix between 40 and 50 K and formation of an HMT film. The spectra of this residual HMT film taken at 100 and 200 K differ slightly from the spectra of the pure solid deposited at 12 K and subsequently warmed to 100 and 200 K. For example, the  $\nu_{22}$  CN stretch of the pure solid deposited directly on the window is a symmetric peak centered at 1005.7  $\text{cm}^{-1}$ , but for the residual film it appears as two peaks at 1007.3 and 1012.5  $\text{cm}^{-1}$ . Differences of this type observed in the spectra of other molecules have been attributed to the effect of variations in the size and shape of the microcrystals (produced on sublimation of the argon) on long-range dipole interactions.<sup>13</sup>

**TABLE 2: HMT Photoproduct Peak Positions and Assignments<sup>a</sup>**

matrix	12 K + UV	after 100 K warm up	after 200 K warm up	assignment
argon	664.5 vw	664.5		CO <sub>2</sub>
		866.6 (broad)	869.4	HN=C=NH or N(CH <sub>3</sub> ) <sub>3</sub>
	903.4 w			Ar <sub>2</sub> H <sup>+</sup>
	1039.9 vw	1039.9 vw		NH <sub>3</sub> or N(CH <sub>3</sub> ) <sub>3</sub>
	1142.9 vw		1142.2	CH <sub>3</sub> NH <sub>2</sub>
	1181.7 vw	1181.7 vw	1180.8	CH <sub>3</sub> NH <sub>2</sub>
	1304.3 vw			CH <sub>4</sub>
		2090.3 vw		?
		2098.8 vw		HN=C=NH
	2138.7 w			CO
	~2161 <sup>b</sup> vw			RNC
		2254.9 vw		RCN (HNCO)
		2263.1 w		H <sub>2</sub> NCN (HNCO)
		2311.4 w		carbonsuboxide or malononitrile?
	H <sub>2</sub> O	2345.2	2345.2	
663.4		658.2 (broad)		CO <sub>2</sub>
667.8		667.8 vw		CO <sub>2</sub>
922.4 vw		922.4 vw		RNC
984.0 <sup>c</sup>				
1038.9		1038.9 w		NH <sub>3</sub> or N(CH <sub>3</sub> ) <sub>3</sub>
1305.6 vw		1301.3 vw		CH <sub>4</sub>
1415.1 vw				CH <sub>3</sub> NO or CH <sub>2</sub> NO <sub>2</sub>
1451.2 vw				CH <sub>3</sub> NO or CH <sub>2</sub> NO <sub>2</sub>
2139.7 w		2136.0 vw		CO
2172.5 w		2169.4 vw	2157.5 vw	RNC
2234.3 w		2230.6 vw		RCN? (HNCO)
2263.0 w		2263.1 w		H <sub>2</sub> NCN
2279.8 w		2275.2 vw		HOCN (HNCO)
		2308.9 vw		carbonsuboxide or malononitrile?
2344.6 s	2340.4 s		CO <sub>2</sub>	

<sup>a</sup> Assignments are tentative and are based solely on proximity to bands reported in the literature. See text for the relevant references. The total irradiation time was 9 h for the HMT-Ar sample and 14 h for the HMT-H<sub>2</sub>O sample. <sup>b</sup> This band was apparent after 90 min of photolysis, but after 9 h of photolysis it had decreased in strength. <sup>c</sup> Band visible after 90 min of irradiation, but was gone after 14 h of irradiation.

As the HMT-H<sub>2</sub>O mixture was warmed from 12 to 100 K, the positions of most of the features attributed to HMT remained essentially unchanged ( $\pm 2$  cm<sup>-1</sup>), with the possible exceptions

being the CH stretching bands in the 2900 cm<sup>-1</sup> region. At 100 K, these were obscured by the shoulder of the asymmetric OH stretching band of H<sub>2</sub>O. By 200 K, the H<sub>2</sub>O had sublimed away, leaving a film of HMT which produces bands essentially identical to those of solid HMT at that temperature.

**Photolysis of HMT in an Argon Matrix.** All the bands attributed to HMT isolated in argon at 12 K diminish upon UV irradiation of the sample with the hydrogen lamp (Figure 2a,b). After 9 h of irradiation, the loss of starting material was accompanied by the growth of new spectral features. Further spectral changes were seen when the sample was warmed to 100 and 200 K after photolysis (Figure 2c,d). The changes in the spectrum during photolysis and subsequent warm up of the sample are summarized in Table 2.

A number of small peaks were formed during photolysis of HMT in argon and can be assigned. The peak at 903.4 cm<sup>-1</sup> observed in the argon matrix after brief photolysis is caused by HAR<sub>2</sub><sup>+</sup>.<sup>14</sup> Such protons are quite mobile, and as expected, this species does not survive annealing to 100 K. The weak feature seen near 2161 cm<sup>-1</sup> may be the result of the presence of an isonitrile or unusual nitrile compound (*vide infra*). This species is photosensitive, as continued exposure to UV radiation causes it to disappear. Continued irradiation also produces new bands at 2345.2, 2138.7, and 664.5 cm<sup>-1</sup>, due to CO<sub>2</sub>,<sup>15</sup> CO,<sup>16</sup> and CO<sub>2</sub>,<sup>15</sup> respectively. The abundance of these oxides is very small and is consistent with the oxygen being derived from trace amounts of H<sub>2</sub>O (<2% of the concentration of HMT in the matrix) present in the argon matrix prior to irradiation and measured by weak bands near 1624 and 1607 cm<sup>-1</sup>.

Some very weak features were also observed following photolysis. The 1304.3 cm<sup>-1</sup> band is most likely due to CH<sub>4</sub>.<sup>17</sup> Bands near 2311 cm<sup>-1</sup> were observed in studies of carbon suboxide and malononitrile in inert gas matrices,<sup>18</sup> but were not assigned. Either carbon suboxide or malononitrile could have been generated under these conditions, and the feature at 2311.4 cm<sup>-1</sup> remains unidentified. The peak at 2263.1 cm<sup>-1</sup> is probably H<sub>2</sub>N-CN<sup>19</sup> and the band at 2254.9 cm<sup>-1</sup> a simple alkyl nitrile.<sup>20</sup> The weak feature at ~2170 cm<sup>-1</sup> and the very weak

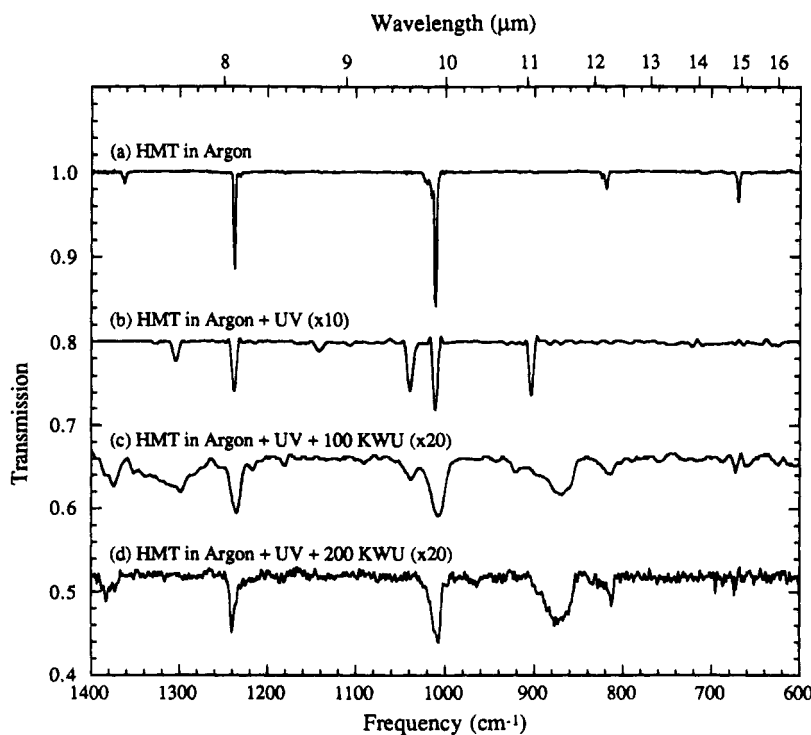


**Figure 2.** 1400–600 cm<sup>-1</sup> infrared spectra of (a) HMT in argon at 12 K, (b) HMT photolyzed in argon at 12 K, (c) HMT photolyzed in argon at 12 K and subsequently warmed to 100 K, and (d) HMT photolyzed in argon at 12 K and subsequently warmed to 200 K.

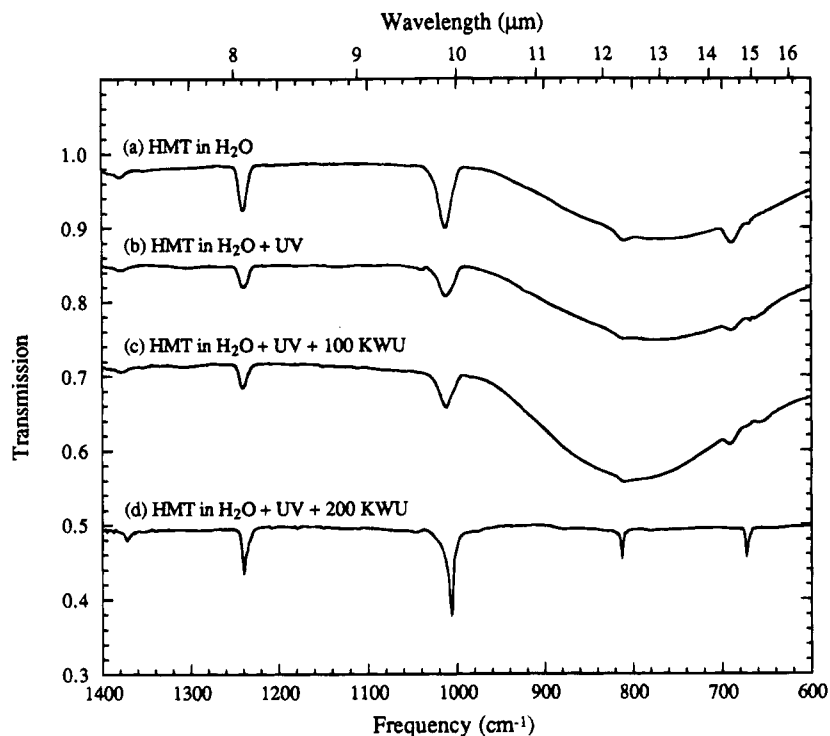


**Figure 3.** 1400–600  $\text{cm}^{-1}$  infrared spectra of (a) HMT in  $\text{H}_2\text{O}$  at 12 K, (b) HMT photolyzed in  $\text{H}_2\text{O}$  at 12 K, (c) HMT photolyzed in  $\text{H}_2\text{O}$  at 12 K and subsequently warmed to 100 K, and (d) HMT photolyzed in  $\text{H}_2\text{O}$  at 12 K and subsequently warmed to 200 K.

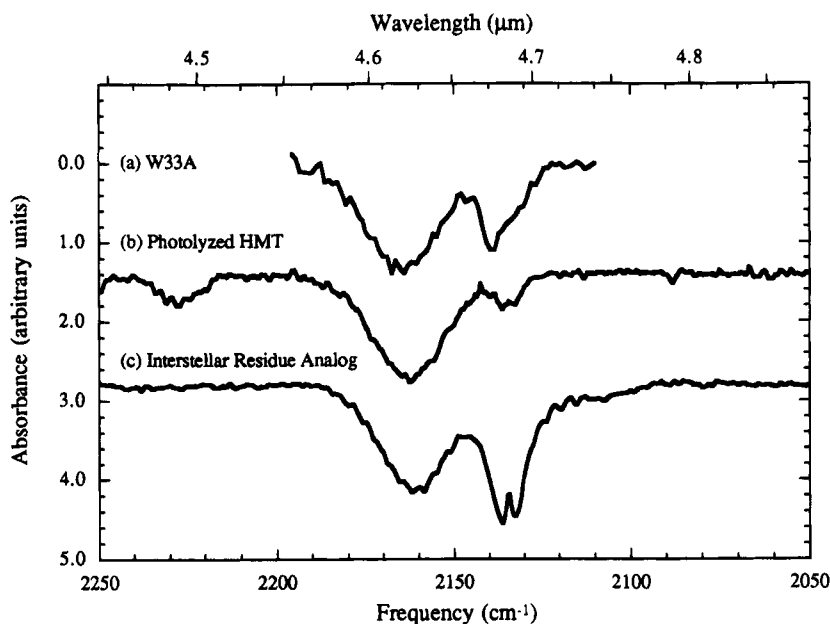


**Figure 4.** 2250–2050  $\text{cm}^{-1}$  infrared spectra of (a) W33A, a protostar deeply embedded in an interstellar cloud of dust, gas, and ice (see ref 23), (b) HMT photolyzed in  $\text{H}_2\text{O}$  at 12 K and subsequently warmed to 150 K, and (c) an astrophysical dust analog consisting of an  $\text{H}_2\text{O}/\text{CH}_3\text{OH}/\text{CO}/\text{NH}_3 = 20:10:1:1$  ice photolyzed at 12 K and subsequently warmed to 150 K (these residues are known to contain HMT, see ref 9).

feature at 922.4  $\text{cm}^{-1}$  are consistent with the N–C and  $\text{R}_3\text{C}-\text{N}$  stretches of an isonitrile, such as  $\text{CH}_3\text{NC}$ .<sup>21</sup> Tentative additional assignments include  $\text{CH}_3\text{NH}_2$  for the bands at 1180.8 and 1142.9  $\text{cm}^{-1}$ <sup>22</sup> and  $\text{N}(\text{CH}_3)_3$  for the bands at 1039.9 and perhaps 866.6  $\text{cm}^{-1}$ .<sup>23,24</sup> Alternatively, the 1039.9  $\text{cm}^{-1}$  band could be due to  $\text{NH}_3$ ,<sup>25</sup> and the 2098.8 and 866.6  $\text{cm}^{-1}$  bands may be due to  $\text{HN}=\text{C}=\text{NH}$ .<sup>19</sup>

A summary of the new bands formed during photolysis and warm up, and their tentative identifications, can be found in Table 2.

**Photolysis of HMT Frozen in  $\text{H}_2\text{O}$ .** The photolysis of HMT frozen in  $\text{H}_2\text{O}$  at 12 K causes reduction of the bands assigned to HMT (Figure 3a,b), although not as rapidly as photolysis in argon, and the production of new features. Under these

conditions, the disappearance of HMT had a half-life on the order of 10 h (as opposed to the half-life of  $\sim 30$  min for HMT in argon). As with the HMT–Ar sample, further spectral changes were seen when the sample was warmed to 100 and 200 K after photolysis (Figure 3c,d), and these are summarized in Table 2.

Identification of the peaks formed during photolysis of HMT in  $\text{H}_2\text{O}$  is somewhat more problematical since interactions with the  $\text{H}_2\text{O}$  generally produce large band shifts and there are few published studies of candidate species frozen in  $\text{H}_2\text{O}$ . Nonetheless, by analogy to the results for HMT in argon, and comparison with what literature on  $\text{H}_2\text{O}$ -rich ices is available, we can tentatively assign a number of the peaks formed during photolysis of HMT in  $\text{H}_2\text{O}$ . As with the HMT in argon, the

strong photoproduct features at 2344.6, 2139.7, 1305.6, and 663.4  $\text{cm}^{-1}$  are certainly due to  $\text{CO}_2$ ,  $\text{CO}$ ,  $\text{CH}_4$ , and  $\text{CO}_2$ , respectively. As noted above, the weak feature at  $\sim 2309$  may indicate the formation of carbon suboxide or malononitrile. The bands between 2300 and 2100  $\text{cm}^{-1}$  are probably all caused by CN stretches.<sup>20</sup> The 2279.8  $\text{cm}^{-1}$  feature may be HOCN,<sup>26</sup> the peak at 2263.0  $\text{cm}^{-1}$  is probably  $\text{H}_2\text{NCN}$ ,<sup>19</sup> and the band at 2234.3  $\text{cm}^{-1}$  is a simple alkyl nitrile, RCN,<sup>20,25</sup> although the peaks at both 2279.8 and 2234.3  $\text{cm}^{-1}$  could instead be caused by HNCO.<sup>26</sup> The band at 1038.9  $\text{cm}^{-1}$  was assigned to  $\text{N}(\text{CH}_3)_3$  or  $\text{NH}_3$  above when observed in the argon matrix, but here it may also be  $\text{O}_3$  generated from photolysis of  $\text{H}_2\text{O}$ .<sup>23,25</sup> In contrast to the photolysis of HMT in argon, HMT photolyzed in  $\text{H}_2\text{O}$  does not appear to produce the 1180.8 and 1142.9  $\text{cm}^{-1}$  bands tentatively identified with  $\text{CH}_3\text{NH}_2$ , perhaps because the nitrogen is oxidized. In this regard, we note that the bands at 1451.2 and 1415.1  $\text{cm}^{-1}$  are consistent with  $\text{N}=\text{O}$  asymmetric stretches and  $\text{CH}_2$  or  $\text{CH}_3$  asymmetric deformations, respectively, in molecules such as  $\text{CH}_3\text{NO}$  and  $\text{CH}_2\text{NO}_2$  isolated in argon.<sup>27</sup>

The photoproduction of a peak at 2172.5  $\text{cm}^{-1}$  may have important astrochemical implications. A feature in the neighborhood of 2160  $\text{cm}^{-1}$  has been observed in the absorption spectra of dense molecular clouds surrounding protostars in the interstellar medium (Figure 4a).<sup>28,29</sup> Bands observed in this (2160–2170  $\text{cm}^{-1}$ ) region of the spectrum are consistent with certain CN triple bonds, although considerably below the normal range for most nitriles, and could be caused by an unusual nitrile or an isonitrile.<sup>28,29</sup> A very similar feature is produced upon photolysis of HMT in  $\text{H}_2\text{O}$  (Figure 4b). At least as early as 1970, HMT was suggested to be a constituent of the interstellar medium.<sup>6</sup> Subsequently, HMT has been produced in laboratory experiments which approximate conditions in the interstellar medium,<sup>7,9,10,30</sup> and recently HMT has been considered in models of cryovolcanic lava flows on icy planets.<sup>8</sup>

## Summary

We have demonstrated that hexamethylenetetramine (HMT,  $\text{C}_6\text{H}_{12}\text{N}_4$ ) can be isolated in matrices using a fairly simple experimental technique, thus opening up a wide range of possible future studies. The infrared spectra of HMT at 12 K isolated in argon and  $\text{H}_2\text{O}$ , and in pure form, have been reported. The results of ultraviolet photolysis of matrix-isolated HMT and HMT frozen in  $\text{H}_2\text{O}$  ice have also been presented and some of their implications for infrared astronomy and astrochemistry discussed. In particular, a photoproduct of HMT may be responsible for the interstellar 2160  $\text{cm}^{-1}$  absorption feature.

**Acknowledgment.** This work was supported by NASA Grants 452-33-93-03 (Origins of Solar Systems Program) and 185-52-12-04 (Exobiology Program). The authors are grateful for useful discussions with R. B. Bohn, D. Hudgins, and B. Khare and helpful advice from reviewers.

## References and Notes

(1) SETI Institute postdoctoral research associate.

- (2) Bulterov, A. *Ann.* **1859**, *11*, 250. Walker, J. F. *Formaldehyde; Reinhold*: New York, 1964; p 511. Smolin, E. M.; Rapoport, L. *S-Triazines & Derivatives*; Interscience: New York, 1959; p 545.
- (3) Dickinson, R. G.; Raymond, A. L. *J. Am. Chem. Soc.* **1923**, *45*, 22.
- (4) Bertie, J. E.; Solinas, M. *J. Chem. Phys.* **1974**, *61*, 1666.
- (5) Mecke, R.; Mathieu, J. P. *J. Chem. Phys.* **1956**, *53*, 106.
- (6) Sagan, C.; Khare, B. N. *Bull. Am. Astron. Soc.* **1970**, *2*, 340. Khare, B. N.; Sagan, C. *Proceedings of the Symposium on Spectroscopic Studies of Astrophysical Interest*, Hyderabad, 1972; p 13.
- (7) Schutte, W. A. Ph.D. Dissertation, Univ. of Lieden, 1988.
- (8) Kargel, J. S. *Icarus* **1992**, *100*, 556.
- (9) Our studies demonstrating the UV photoproduction of HMT in methanol-containing cometary and interstellar ice analogs will be submitted to the journal *Astrophys. J.* in the near future.
- (10) Allamandola, L. J.; Sandford, S. A.; Valero, J. G. *Icarus* **1988**, *76*, 225.
- (11) Warnek, P. *Appl. Opt.* **1962**, *1*, 721.
- (12) Hudgins, D. M.; Allamandola, L. J.; Sandford, S. A. In Preparation for submission to *J. Phys. Chem.*
- (13) Ovchinnikov, M. A.; Wight, C. A. *J. Chem. Phys.* **1993**, *99*, 3374.
- (14) Wight, C. A.; Ault, B. S.; Andrews, L. *J. Chem. Phys.* **1976**, *65*, 1244. Bondybey, V. E.; Pimentel, G. C. *J. Chem. Phys.* **1972**, *56*, 3832. Milligan, D. E.; Jacox, M. E. *J. Mol. Spectrosc.* **1973**, *46*, 460. Andrews, L.; Ault, B. S.; Grzybowski, J. M.; Allen, R. O. *J. Chem. Phys.* **1975**, *62*, 2461.
- (15) Irvine, M. J.; Mathieson, J. G.; Pullin, A. D. E. *Aust. J. Chem.* **1982**, *35*, 1971. Sandford, S. A.; Allamandola, L. J. *Astrophys. J.* **1990**, *355*, 357.
- (16) Jiang, G. J.; Person, W. B.; Brown, K. G. *J. Chem. Phys.* **1975**, *62*, 1201. Sandford, S. A.; Allamandola, L. J.; Tielens, A. G. G. M.; Valero, J. G. *J. Astrophys. J.* **1988**, *329*, 498.
- (17) Cabana, A.; Savitsky, G. B.; Hornig, D. F. *J. Chem. Phys.* **1963**, *39*, 2942. Milligan, D. E.; Jacox, M. E. *J. Chem. Phys.* **1967**, *47*, 5157.
- (18) Ames, L. L.; White, D.; Mann, D. E. *J. Chem. Phys.* **1963**, *38*, 910.
- (19) Krantz, A.; Laureni, J. *J. Am. Chem. Soc.* **1981**, *103*, 486. King, S. T.; Strope, J. H. *J. Chem. Phys.* **1971**, *54*, 1289.
- (20) Streitwieser, A., Jr.; Heathcock, C. H. *Introduction to Organic Chemistry*; MacMillan: New York, 1981.
- (21) Freedman, T. B.; Nixon, E. R. *Spectrochim. Acta A* **1968**, *28A*, 1375.
- (22) Durig, J. R.; Bush, S. F.; Baglin, F. G. *J. Chem. Phys.* **1968**, *49*, 2106.
- (23) Goldfarb, T. D.; Khare, B. N. *J. Chem. Phys.* **1967**, *46*, 3379.
- (24) Methylamines have been observed in the thermal decomposition of HMT: Iwakami, Y.; Takazono, M.; Tsuchiya, T. *Bull. Chem. Soc. Jpn.* **1968**, *41*, 813.
- (25) d'Hendecourt, L. B.; Allamandola, L. J. *Astron. Astrophys. Suppl. Ser.* **1986**, *64*, 453. Unpublished results in our lab put  $\text{O}_3$  in  $\text{H}_2\text{O}$  at 1035  $\text{cm}^{-1}$  at 12 K.
- (26) Jacox, M. E.; Milligan, D. E. *J. Chem. Phys.* **1964**, *40*, 2457.
- (27) Jacox, M. E. *J. Chem. Phys.* **1983**, *87*, 3126. Barnes, A. J.; Hallam, H. E.; Waring, S.; Armstrong, J. R. *J. Chem. Soc., Faraday Trans. 2* **1976**, *72*, 1.
- (28) Lacy, J. H.; Baas, F.; Allamandola, L. J.; Persson, S. E.; McGregor, P. J.; Lonsdale, C. J.; Geballe, T. R.; van der Bult, C. E. P. *Astrophys. J.* **1984**, *276*, 533.
- (29) Tegler, S. C.; Weintraub, D. A.; Allamandola, L. J.; Sandford, S. A.; Rettig, T. W.; Campins, H. *Astrophys. J.* **1993**, *411*, 260. Larson, H. P.; Davis, D. S.; Black, J. H.; Fink, U. *Astrophys. J.* **1985**, *299*, 873.
- (30) Argarwal, V. K.; Schutte, W.; Greenberg, J. M.; Ferris, J. P.; Briggs, R.; Connor, S.; Van de Bult, C. P. E. M.; Baas, F. *Origins Life Evol. Biosphere* **1985**, *16*, 21. Briggs, R.; Ertem, G.; Ferris, J. P.; Greenberg, J. M.; McCain, J. P.; Mendoza-Gomez, C. X.; Schutte, W.; *Origins Life Evol. Biosphere* **1992**, *22*, 287.